frontiers | Frontiers in Mechanical Engineering

TYPE Original Research
PUBLISHED 28 October 2022
DOI 10.3389/fmech.2022.1005646

OPEN ACCESS

EDITED BY
Mohd Khir Mohd Nor,
Universiti Tun Hussein Onn Malaysia, Malaysia

REVIEWED BY
Jitendra Kumar Katiyar,
SRM Institute of Science and Technology, India
Dirk Pons,
University of Canterbury, New Zealand

*CORRESPONDENCE
Tri Widodo Besar Riyadi,
Tri.Riyadi@ums.ac.id

SPECIALTY SECTION
This article was submitted to Solid and Structural Mechanics, a section of the journal Frontiers in Mechanical Engineering

RECEIVED 28 July 2022
ACCEPTED 11 October 2022
PUBLISHED 28 October 2022

CITATION
Riyadi TWB, Siswanto WA and Zhu X (2022), Interfacial formation of intermetallic Ni-Al-Ti systems formed by induction heating.
Front. Mech. Eng 8:1005646.
doi: 10.3389/fmech.2022.1005646

Interfacial formation of intermetallic Ni-Al-Ti systems formed by induction heating

Tri Widodo Besar Riyadi[1]*, Waluyo Adi Siswanto[1] and Xiaomeng Zhu[2]

[1]Faculty of Engineering, Universitas Muhammadiyah Surakarta, Surakarta, Jawa Tengah, Indonesia, [2]School of Materials Science and Engineering, Wuhan University of Technology, Wuhan, China

Intermetallic systems of Nickel (Ni), Aluminium (Al), and Titanium (Ti) are candidates for lightweight materials that offer high-temperature resistance. Combustion synthesis has been widely studied to produce intermetallic and coating deposition by exploiting the heat released by the combustion. An underlayer is often used to enhance the adhesion of the coating to the substrate. The interaction of the coating and the underlayer during heating is, therefore, crucial for achieving a good adhesion quality. This work aimed to investigate the microstructure and properties of the interfacial formation across the NiAl coatings and Ti underlayers formed by combustion synthesis. Induction heating was used to initiate the heating and reaction process with heating rates of 46.6, 57.0, and 85.5 K/s. The microstructure was characterized by Scanning Electron Microscopy (SEM) equipped with an Energy Dispersive Spectroscopy (EDS) detector, whereas the formed phases were identified using X-ray Diffraction (XRD) tests. The hardness distribution was measured by the Vickers microhardness test. The result shows that NiAl with Al-rich and Ni-rich were formed in the coating region. The average thickness of the coating increases by approximately 200, 300, and 400 μm with a heating rate of 46.6, 57.0, and 85.5 K/s, respectively. The different thicknesses of the coating can be attributed to the migration of Ni/Al from the coating to the underlayer zones. The microstructure observed in the underlayer confirms the formation of several intermetallic phases of Ni-Ti and Ti-Al systems. The infiltration of Ni and Al elements from Ni and Al to Ti sides was responsible for generating a reaction between Ni-Ai-Ti. The formation of Ti_2Ni–Ti_3Al phases in the underlayer increases with the heating rate. The hardness across the coating, interface, and underlayer increases with the heating rates. The heating rate of 46.6, 57.0, and 85.5 K/s results in the hardness of the interface by 669.1, 804.8, and 967.7 HV, whereas the underlayer increases by 680.1, 772.7, and 978.7 HV, respectively. The increased content of the Ni-Al-Ti system, which are $AlNi_2Ti$ and Ti_2Ni–Ti_3Al phases, was attributed to the increased hardness of the interface and underlayer. This work improves the understanding of second reactions across the interface while fabricating coatings that apply an underlayer.

KEYWORDS

NiAl-Ti, combustion synthesis, interfacial microstructure, hardness distribution, underlayer

1 Introduction

The development of a hypersonic vehicle for space applications has demanded using a specific material with specifications for high thermal stability, low structural weight, and compatibility with high temperatures A high strength-to-weight ratio and elevated turbine entrance temperature are necessary to develop a lightweight, effective turbine for aircraft engine applications to provide more thrust. Improved fuel economy in automobiles results from weight savings from using lightweight materials. Ti_3Al and TiAl intermetallics with low density and good thermal conductivity appeal to the auto industry, which needs heat resistance for engine parts that turn at high speeds (Djanarthany et al., 2001). Other intermetallic materials, such as NiAl and $MoSi_2$, are also widely investigated for high-temperature applications.

Intermetallic is a term used to describe a compound or phase that synthesizes two or more metals in a particular proportion and has a distinct crystalline structure from its constituents (Sauthoff, 2008). Intermetallics' main benefit is that they have long-range structured crystal structures, which reduces the difficulties of dislocation motion. Intermetallics can have good properties in high temperatures, such as a high melting point and good strength, but suffer in low temperatures, such as brittleness and fracture toughness, due to this factor (Stolo et al., 2000). Table 1 illustrates the properties of some intermetallics' melting points and densities.

TABLE 1 Properties of some intermetallics (Cinca and Guilemany, 2012).

Intermetallic compounds	Melting point (°C)	Density (kg/m^3)
NiAl	1,640	5.86×10^3
Ni_3Al	1,390	7.50×10^3
FeAl	1,250	5.56×10^3
Fe_3Al	1,540	6.72×10^3
TiAl	1,460	3.91×10^3
Ti_3Al	1,600	4.2×10^3
$TiAl_3$	1,350	3.4×10^3

TABLE 2 Chemical composition (in at%) of the phases in Figure 3.

Spot	Al	Ti	Ni	Possible phase
A	54.65		45.35	NiAl (Al-rich)
B	42.47		57.53	NiAl (Ni-rich)
C	15.53	83.36	1.11	Ti_3Al
D	7.88	60.37	31.27	Ti_2Ni
E	2.04	94.57	3.39	Ti Alloy

Due to their high melting temperatures and superior oxidation resistance, NiAl and TiAl have been widely considered potential materials for high-temperature applications among various intermetallic compounds (Cinca and Guilemany, 2012). Compared to its constituent elements, Ni (1728 K) and Al (933 K), the NiAl phase has a higher melting point (1911 K). This property shows that the atomic bonds between the dissimilar Ni and Al atoms are significantly stronger than those between the similar Al and Ni atoms. The crystal structure of NiAl is substantially distinct from that of its constituents. NiAl has a B2 structure, which is a bcc structure with atomic ordering, whereas Ni and Al have an fcc structure (Sauthoff, 2008).

Djanarthany et al. (Djanarthany et al., 2001) investigated various methods for fabricating Ti_3Al and TiAl, including ingot metallurgy, reactive sintering or combustion synthesis, and explosive shock-wave consolidation. Combustion synthesis has grown increasingly attractive in recent decades as a method of producing intermetallics since it offers many significant advantages. After the ignition, the combustion reaction will self-propagate itself. Other layers will ignite in response to the heat generated by the front layer's combustion. The process can be made much more efficient by removing the additional heat source needed by other techniques to maintain the combustion process (Moore and Feng, 1995). The highly exothermic nature of the combustion reaction ensures that the combustion process is completed. The high combustion synthesis temperature may exceed some elemental impurities' low boiling point. Because of this, contaminants can be boiled during the combustion reaction, improving product purity. The rapid combustion rate achieves better homogeneity of the finished product. The heat loss is reduced by rapid heating, which causes the reaction to be completed and generates a homogeneous microstructure. In conclusion, because the reaction happens fast, the process becomes more efficient, using less energy (Merzhanov, 1996). Initiating a combustion reaction with enough energy is made possible by the ignition technique (Moore and Feng, 1995). It has been documented that current heat sources, including induction heating, microwave, and laser, can initiate combustion synthesis. Since induction heating generates heat from within the material, it offers substantial benefits for enhancing the efficiency and completeness of the combustion reaction. An area of an electrically and magnetically conductive substance can be heated by induction heating, which also has the advantages of being rapid and contactless, accurate, repeatable, clean, and environmentally safe.

Given that it only involves one step of processing, the synthesis and deposition of coatings with combustion synthesis have gained popularity (Merzhanov, 1996), (Morsi, 2001), (Gao et al., 2013a). However, the high temperature of the combustion reaction creates difficulties for the coating and substrate to adhere to one another. It has been demonstrated that the exothermic reaction's high temperature induces a thermal shock, causing high thermal stress. The coatings might separate from the substrate and generate cracks due to the high thermal stress. Reducing the thermal stresses using an underlayer can improve the bonding of the coating (Riyadi et al., 2014a), (Riyadi et al., 2016).

A prior study successfully used combustion synthesis to fabricate a NiAl coating onto a steel substrate. However, the Ni-Al combustion reaction's high temperature promotes Ni and Al element infiltration and mixing in the Ti region (Riyadi et al., 2014b). The need for additional research to explore how heating processes affect mixing, which impacts the structure and properties of the interfacial area, follows. This research's objectives were to investigate the interfacial microstructure and properties of the NiAl/Ti bilayer structure ignited by induction heating at various heating rates. The result of this work is expected to advance our understanding of how metal interactions at the interface during combustion synthesis affect structure and property change.

2 Methods

Aluminium (45 m, 99.7%), nickel carbonyl type-123 (4.5 m, 99.85%), and titanium (106 m, 99.46%) were the powder materials used in this study and were supplied by William Rowland United Kingdom. The sample was composed of two layers; the top layer was a Ni-Al mixture with an atomic ratio of 1:1. The mass of the Ni-Al mixture for each sample is 0.5 g. The underlayer is Ti, with a mass of 0.3 g. A steel substrate was manufactured from commercial steel with a diameter of 16 mm and a thickness of 3 mm. A cylindrical die with an inside diameter of 16.0 mm was used to press the mixture to become a pellet. Firstly, the steel substrate was put inside the die container. The Ti powder was then filled into the container and pressed using a pressure of 200 MPa. Subsequently, the Ni/Al powder mixture was filled into the die container above the compacted Ti in the first layer and pressed again using the same pressure used for Ti. The compressed pellet composed of Ti and Ni-Al was then ejected from the die and subsequently inserted into a combustion chamber containing the induction heating coil at a distance of approximately 3 mm from the pellet surface. Figure 1 shows the schematic diagram of the combustion chamber used to carry out the combustion reaction.

An induction heater (2 kW, Cheltenham, United Kingdom) was used to initiate the combustion reaction of the bilayer system with currents of 200 A, 250 A, and 300 A. The different currents of induction heating were used to produce varied heating rates. After the measurement of the temperature profile, the heating rate of the related currents is 46.6, 57.0, and 85.5 K/s. The temperature measurement was conducted using a combination of thermocouple (range from −50–1,100°C) and non-contact infrared pyrometer type Marathon MM (540–3,000°C, manufactured by Raytek®, United Kingdom). The temperature measurement tools were calibrated using a thermometer, as explained in Ref. (Riyadi et al., 2014a). During the combustion reaction, argon gas was kept flowing to avoid oxidation. Induction heating was turned off approximately 1 s after the ignition started. The characterization of the synthesized product began by cutting the samples at their cross sections and mounted using epoxy resin. The surface of the samples was ground using silica papers with rough and smooth grits, polished with diamond paste, and etched using a mixture of methanol/nitrite acid with a 98/2 volume fraction. The phase identification of the products was carried out by XRD (RINT2000 vertical Goniometer) using a scanning rate of 4 deg./min. The microstructure observations were conducted by SEM and EDX (Zeiss EVO50, Germany). A Vickers indentation tester was used to measure the hardness distribution across the product using a load of 0.1 N for 15 s.

3 Results and discussion

3.1 Phase formations

A sample synthesized using a heating rate of 200 A was selected to identify the formed phase of the synthesized product. Figure 2A shows the XRD spectra observed in the coating region at a depth of approximately 40 μm below the coating surface. The XRD spectra show the formation of NiAl, $Ni_{0.58}Al_{0.42}$, $Ni_{0.9}Al_{1.1}$, and Ni_2Al_3 representing the formed phases in the coating region. The appearance of $Ni_{0.58}Al_{0.42}$ and $Ni_{0.9}Al_{1.1}$ phases can be related to the infiltration of Ni and Al from NiAl to Ti regions. The high spectra intensity of the $Ni_{0.58}Al_{0.42}$ shows the high content of NiAl with Ni-rich, indicating that the migration of Al liquid is higher than that of Ni liquid. The lower melting point of Al is responsible for the faster diffusion of Al. At the same time, the formation of Ni_2Al_3 can be related to the incomplete reaction. The low heating rate leads to insufficient energy to complete the SHS process of Ni/Al.

Figure 2B shows the XRD spectra observed in the underlayer at a depth of approximately 600 μm below the coating surface. The result shows that several phases consisting of Ti_3Al, Ti_2Ni, Ti, Fe_2Ti_4O, and $AlNi_2Ti$ were formed in the underlayer region. The formation of Ti_2Ni and Ti_3Al demonstrates a diffusion of Al and Ti from the NiAl region to the Ti region, which then reacts with Ti to form Ti–Ni

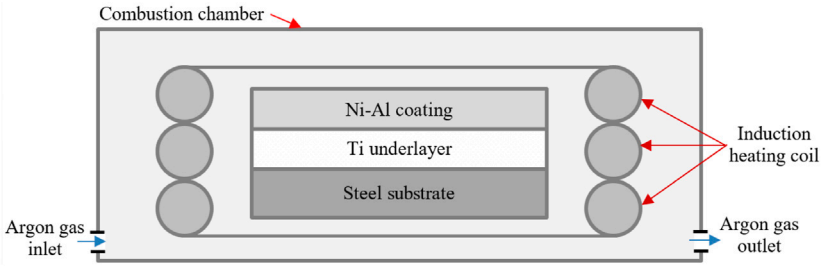

FIGURE 1
The schematic figure of combustion chamber containing induction heating.

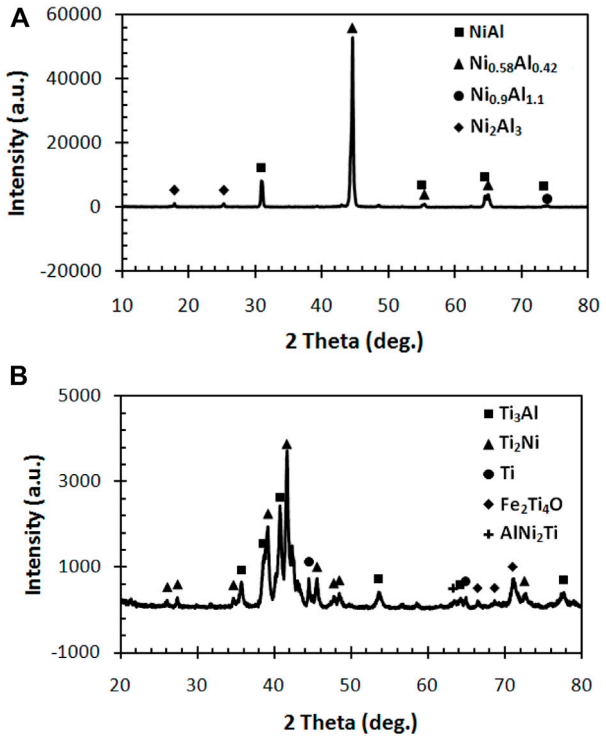

FIGURE 2
XRD spectra identified at **(A)** coating, and **(B)** underlayer.

and Ti–Al systems. Whereas the formation $AlNi_2Ti$ indicates the reaction of the Ni–Al–Ti system. The presence of Ti suggests the existence of unreacted Ti. In contrast, the appearance of Fe_2Ti_4O can be attributed to the formation of oxides due to the oxidation reaction between the diffused oxygen into the underlayer, Ti underlayer, and the melted Fe substrate. Different sources of oxygen can exist during a combustion synthesis, such as the compacted pellet and the entrapped gas. In comparison, the melted Fe can be caused by the heat released by Ni/Al reaction and the heat generated by induction heating.

3.2 Microstructure

Induction heating with various heating rates was used to initiate the combustion synthesis of the compacted pellet composed of the Ni-Al mixture and Ti on a substrate. Figures 3A–C show the typical microstructure of the synthesized products obtained by heating rates of 46.6, 57.0, and 85.5 K/s, respectively. The result shows that the increase of the heating rates by 46.6, 57.0, and 85.5 K/s produces an average coating thickness of approximately 200, 300, and 400 μm, respectively. This result indicates that the coating thickness at a slower heating rate is smaller than that at a faster one. This result suggests that the amount of elemental Ni and Al diffused from the coating to underlayer regions at a slower heating rate is higher than that at a faster heating rate. A possible reason for this might be that the time for diffusion of the elemental Ni and Al into the underlayer region is longer than that at the faster heating rate. According to the EDS analysis in Table 2, the existence of bright and grey areas in the coating region represents the formation of NiAl with Al-rich (spot A) and NiAl with Ni-rich (spot B). The diffusion of Ni and Al from the coating region to the underlayer region is responsible for forming these phases. The EDS analysis of the phases in the underlayer also indicates that several intermetallic phases of the Ti–Ni and Ti–Al systems mainly consist of Ti_2Ni and Ti_3Al. The black phase shown by spot C suggests the formation of the Ti_3Al phase. Around the black phase, spot D, with a grey colour, was identified as Ti_2Ni. This phase proves that there were other reactions between Ni-Al and Ti in the underlayer region. Comparing the formed phases in the underlayer, an increase in the heating rate promotes a higher portion of Ti_2Ni–Ti_3Al phases in the underlayer. A possible explanation for this result might be that when the heating rate is slow, the time needed to melt Ti and initiate the reaction between the Ni-Al and Ti takes longer, which results in a high heat loss. Consequently, the combustion reaction between the Ni-Al and Ti in the underlayer was incomplete. Observation of the SEM image in the underlayer region of the synthesized product prepared by various heating rates also shows that a large area in a dark grey

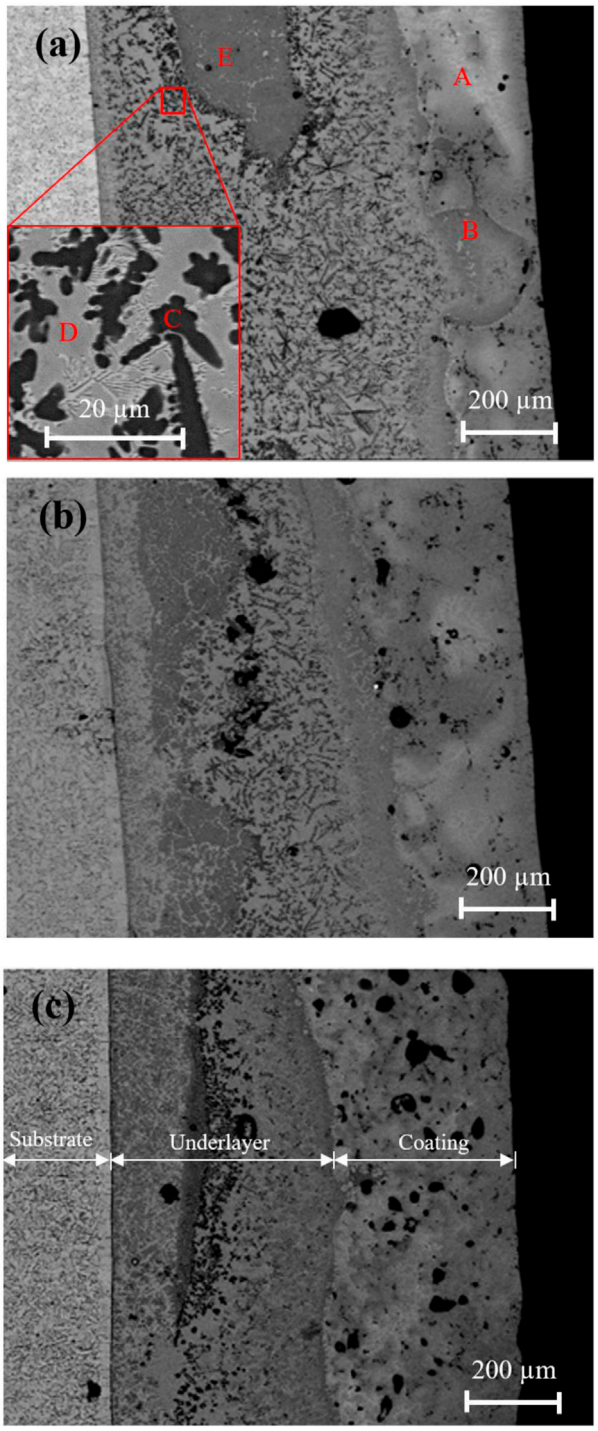

FIGURE 3
Back scattered SEM micrograph of synthesized by heating rates of **(A)** 46.6 K/s, **(B)** 57.0 K/s, and **(C)** 85.5 K/s.

area marked by spot E was observed, particularly in Figure 3A. The elemental composition of spot A, as given in Table 2, indicates that the dark area is attributed to the existence of a Ti alloy. An increase in the heating rates reduces the dark area, showing the smaller Ti alloy formation.

The varying heating rates have affected on the porosity of the synthesized product. The results demonstrate that the number of pores in the synthesized product heated at a higher rate (85.5 K/s) is more significant than those heated at a lower rate (46.6 and 57.0 K/s). Pores in the compacted pellet are the leading causes of porosity in synthesized products (Tay et al., 2008). The Kirkendall effect, which refers to the difference in diffusion rates during solid-state sintering, and the gas evolutions during the phase transformation in the SHS reaction are the additional factors that contribute to the formation of pores (Gao et al., 2013b). This work suggests that the high porosity shown with the higher heating rate was caused by the reaction's short duration, which prevented the holes from rising to the surface in a reasonable timeframe. On the other hand, a longer reaction duration during a slower heating rate resulted in less residual porosity. Based on this finding, it has been shown that a slow heating rate is preferable to a high heating rate in terms of minimizing porosity and improving densification.

3.3 Elemental distributions

The diffusion of atoms was studied by element scanning to determine the phases' evolution across the interface region, notably in the sample heated at heating rates of 46.6 K/s and 57.0 K/s, as shown in Figures 4A,B. By referring to Figures 4A,B, the atomic concentration of Ni and Al gradually decreases from the coating to the underlayer areas. This result shows that the Ni and Al diffusion from the coating to the underlayer regions was very high. The interfacial reactions between Ni-Al, Ti-Al, Ti-Ni, and Ni-Al-Ti that led to the formation of new products were made possible by the significant amounts of Ni and Al diffusions into the Ti region. However, Ti's evolution shows that the Ti concentration drops dramatically from the underlayer to the coating regions. The rapid decrease in Ti concentration suggests that very little Ti diffuses into the coating region. Powder contamination during preparation may be why a trace amount of Ti appears in the NiAl region.

3.4 Microhardness

Figure 5 shows the coating, interface, and underlayer microhardness of the synthesized products prepared by different heating rates. The result shows that the hardness of the coating fluctuated with various heating rates. The hardness fluctuation of the NiAl coatings can be attributed to the migration of Al and Ni liquids from coating to underlayer zones which lead to the formation of NiAl with Ni-rich and Al-rich, with higher and lower hardness, respectively. The hardness of NiAl coatings prepared with high heating rates is higher than that prepared with lower heating rates. A complete

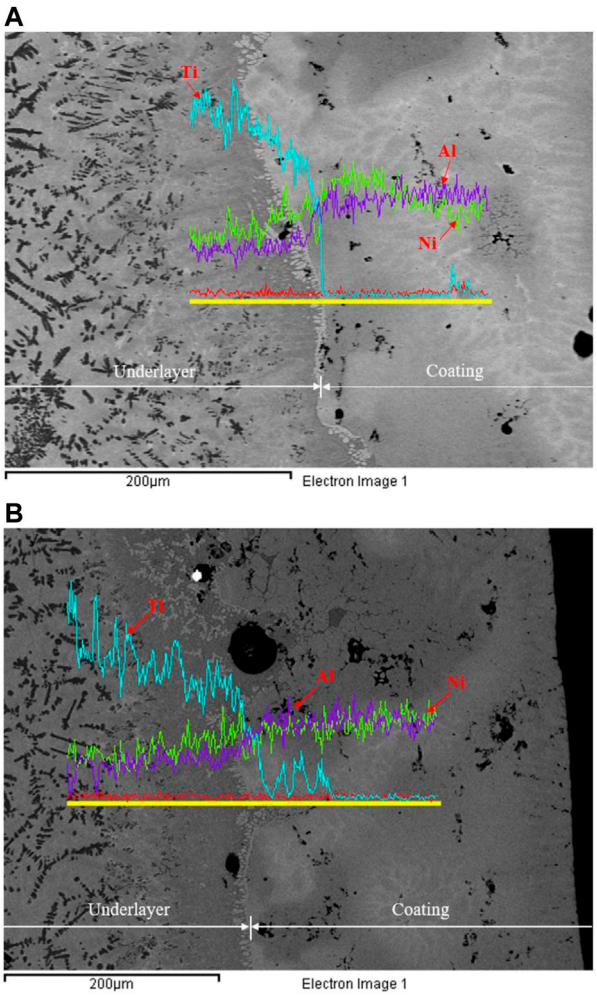

FIGURE 4
Elements distribution across the interface between NiAl and titanium using heating rates of **(A)** 46.6 K/s and **(B)** 57.0 K/s.

reaction between Ni and Al in the high heating rate was responsible for the high hardness. However, the pore content in the product with a high heating rate is sufficiently high. The average hardness of the interface between the NiAl coating and the underlayer indicates is a high increase in the hardness compared to that of the coating. The interface hardness increases with the heating rate. The reaction of the intermetallic system of the Ni-Al-Ti system that forms $AlNi_2Ti$, as verified by XRD in Figures 2B, is responsible for the high hardness of the interface. In the underlayer, an increase in the heating rate increases the hardness of the underlayer. The formation of hard intermetallic phases, mainly comprised of Ti_3Al-Ti_2Ni composites, can be associated with the high hardness in the underlayer region. In contrast, the unreacted Ti that forms Ti alloys shows a lower hardness in the 537–551 HV range. The indentation image over the coating and underlayer regions prepared by a sample with a heating rate of 85.5 K/s is shown in Figure 6 to support the Vickers measurement. Other results of the indentation images show a similar trend. Comparing the stamped pictures across the three regions, the indentation diagonal of the interface region is smaller than that of the coating and the underlayer regions. The smaller the diagonal shows, the higher hardness.

4 Discussion

According to the identification and distribution of the phases and the element distribution in the synthesized product, the microstructure of the coating is mainly composed of NiAl with Al-rich and NiAl with Ni-rich phases. In contrast, the underlayer mainly consists of Ti_3Al and Ti_2Ni phases. Part of the underlayer also contains Ti alloy representing the unreacted Ti. The formation mechanism of the NiAl coating was initiated by the heat generated by the combustion synthesis of Ni-Al that was ignited by induction heating. The synthesized product forms a liquid phase before complete solidification. Due to the effect of capillary action, some of the Ni and Al liquid spread and dispersed through the underlying Ti and began to wet the surface of Ti particles. Due to the lower melting point, Al was melted and spread first before Ni, forming NiAl with Ni-rich in a significant quantity. A small amount of NiAl with Al-rich was also found in the coating because some of the Ni also diffused from the coating region to the underlayer region. The formation of substoichiometric NiAl is possible in the reaction between Ni and Al, as described in the binary phase diagram of Ni–Al (Morsi, 2001).

The diffused Ni-Al liquid to the underlayer covered the solid Ti and produced a new system composed of a Ti, Ni, and Al system. The heat released by the NiAl reaction triggers further reactions of the Ti-Al, Ti-Ni, and Ti-Ni-Al systems. The microstructure analysis revealed that new binary and ternary phases of Ti, Ni, and Al systems were formed in the underlayer. Since the underlayer was initially composed of Ti powders, the formation of Ti_2Ni was attributed to the reaction between Ti and Ni. According to the phase diagram of the binary Ti-Ni system (Salehi et al., 2001), the nickel-titanium system contains the stable TiNi, $TiNi_3$, and Ti_2Ni phases. Ti_2Ni can be formed in the liquid phase at 942°C (1215 K) by eutectic reaction or at 984°C (1257 K) by peritectic reaction (Locci et al., 2003). In the high content of Ti, the final microstructure is Ti_2Ni phase and αTi due to the eutectoidic transformation of βTi-Ni solid solution at 765°C (Cammarota et al., 2009). A study carried out by Li Hai-Xin et al. (Hai-xin et al., 2012) reported that during isothermal solidification of the molten underlayer of the Ti-Ni-Al system (*L*), TiNi was formed first. A peritectic reaction then occurred at 984°C to produce Ti_2Ni and $AlNi_2Ti$. As also reported by Bertolino et al. (Gao et al., 2013a), Ti_2Ni reaction happened in the underlayer after obtaining sufficient energy from the heat released by the synthesis reaction of Ni/Al.

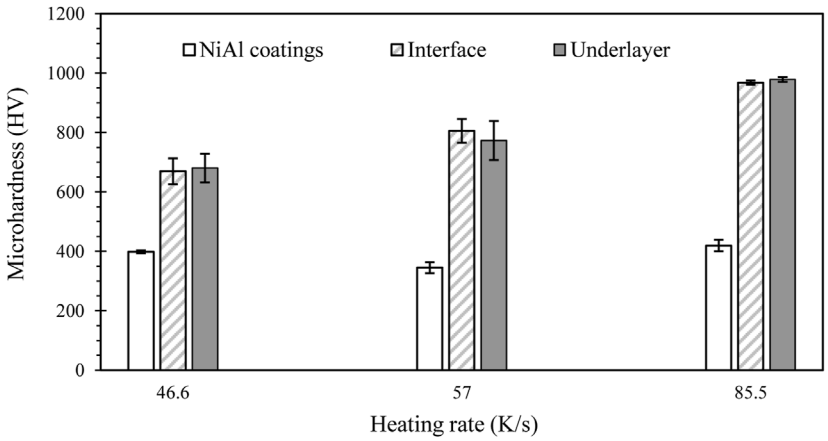

FIGURE 5
Microhardness across the coating, interface, and underlayer with different heating rates.

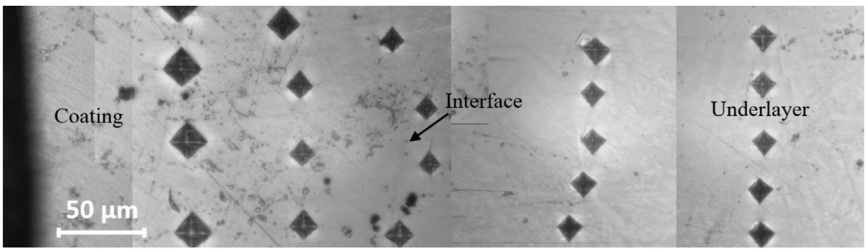

FIGURE 6
Stamped image of Vickers indentations.

The SEM and EDS analysis indicate that the black phase identified as Ti_3Al intermetallic forms a dendrite structure in the Ti_2Ni matrix. The formation of Ti_3Al can happen by the diffusion of Al liquid in the coating into Ti-rich areas in the underlayer. According to the binary phase diagram of the Ti-Al system (Djanarthany et al., 2001), there are six kinds of phases which can appear in the reaction between Ti and Al, which consist of αTi, Ti_3Al (α_2), TiAl (γ), $TiAl_2$, $TiAl_3$ (η) and Al, depending on the composition of Ti-Al and temperature (Djanarthany et al., 2001). Ti_3Al and TiAl have more extensive homogeneity range but cannot be used in a single state because they have low ductility at room temperature. It is proven in this work that Ti_3Al appears around the Ti_2Ni matrix. Shant Prakash Gupta (Gupta, 2002) demonstrated that the liquid Al spread over the surface of Ti particles and formed a layer that covered Ti in the core. Eq. 1 shows the reaction between $TiAl_3$ and the core Ti to produce TiAl. In the final stage, Ti was reduced, and TiAl changed to form Ti_3Al (Orru et al., 1999).

$$Ti + Al_{(liquid)} \rightarrow Ti + TiAl_3 \rightarrow Ti + TiAl_3 + TiAl \rightarrow Ti_3Al \quad (1)$$

A study reported that the reaction of Ti-Al cannot proceed to complete without the assistance of an exothermic agent from the high heat release produced by the previous reaction (Kobashi et al., 2010). In the present work, the exothermic agent was obtained from the heat released by the Ni-Al reaction. Thus, it can be confirmed that the heat released by the Ni-Al reaction has promoted the completion of the Ti-Al reaction to form Ti_3Al. It is still debatable, however, whether the first reaction sequence occurred upon the formation of the Ti-Al system or the Ti-Ni system. Further studies might be required to explore other factors affecting the coating performance, such as the presence of pores and inclusions (Romanova et al., 2020), surface tribology (Ciulli, 2019), corrosion resistance (Darmawan et al., 2022), and the quality of the adhesion (Anggono, 2020). The coating is expected to be used in many applications with higher loads, such as spur gear (Muhammad and Haruna Shanono, 2021) and ballistic panels (Mohd Yuhazri Yaakob et al., 2020).

5 Conclusion

In this work, an induction heater was successfully used to initiate the combustion synthesis of a Ni-Al mixture and a Ti underlayer. Three different currents of induction heating were applied to produce various heating rates. The result shows that all the fabricated coatings firmly adhered to the substrate. The average thickness of the coatings increases by approximately 200, 300, and 400 μm with a heating rate of 46.6, 57.0, and 85.5 K/s, respectively. The different thicknesses of the coating can be attributed to the migration of Ni/Al liquids from the coating to the underlayer zones, which form NiAl with Ni-rich and Al-rich. The diffusion of the elemental Ni and Al from the coating to the underlayer regions at a slower heating rate is higher than that at a faster heating rate. The high temperature released by the combustion synthesis of NiAl in the coating generates further reactions between the diffused Ni and Al liquids and Ti to produce Ti_3Al, Ti_2Ni, and $AlNi_2Ti$ in the underlayer. The intermetallic phase formation increases hardness in the interfacial and the underlayer regions. The average hardness of the interfacial area is 669.1, 804.8, and 967.7 HV, whereas the average hardness of the underlayer is 680.1, 772.7, and 978.7 HV at the heating rate of 46.6, 57.0, and 85.5 K/s, respectively.

The present work has shown that the heating rate plays an essential role in the structure and properties of the synthesized product. A lower heating rate produces a denser coating structure with lower hardness in the underlayer. A lower hardness is, therefore, more preference for the designer to create a denser coating with a softer underlayer. Based on the evidence that the second reaction occurs after the NiAl reaction, further work is recommended to investigate the post-treatment effect on the coating produced by different processes.

Although the present work has been successfully used to study the effect of the heating rate, the performance of coating under a high-temperature environment is not observed yet. A thermal shock test of the NiAl coating is suggested to be carried out for further work. It is also realized that the NiAl coating produced in the present work was prepared using a metal powder which might be costly. Other less expensive processes, such as electroplating and sputtering, might be worth studying.

Data availability statement

The raw data supporting the conclusion of this article will be made available by the authors, without undue reservation.

Author contributions

TR designed the research and all activities. TR and XZ set up the induction heating and sample preparation. The microstructure and mechanical properties of the product were observed by TR using SEM and Vickers microhardness tests, whereas XZ performed the XRD tests. TR wrote the manuscript, and WS contributed to the interpretation of the results and the selection of the journal. All authors discussed and commented on the final version of the manuscript.

Acknowledgments

Great thanks are devoted to Tao Zhang (Kingston University, London, United Kingdom) for his commitment to continuous collaboration. All facilities provided by the Wuhan University of Technology, PR China, are highly appreciated. The authors would like to thank the Directorate General of Higher Education, Ministry of Education and Culture, the Republic of Indonesia, for the financial support provided by Grant No. 072/E5/PG.02.00.PT/2022.

Conflict of interest

The authors declare that the research was conducted in the absence of any commercial or financial relationships that could be construed as a potential conflict of interest.

Publisher's note

All claims expressed in this article are solely those of the authors and do not necessarily represent those of their affiliated organizations, or those of the publisher, the editors and the reviewers. Any product that may be evaluated in this article, or claim that may be made by its manufacturer, is not guaranteed or endorsed by the publisher.

References

Anggono, A. D. (2020). Analysis of mechanical and metallographic properties on the joining between aluminum and brass by using the brazing method. *Int. J. Emerg. Trends Eng. Res.* 8 (2), 440–446. doi:10.30534/ijeter/2020/31822020

Cammarota, G. P., Casagrande, a., Poli, G., and Veronesi, P. (2009). Ni–Al–Ti coatings obtained by microwave assisted SHS: Effect of annealing on microstructural and mechanical properties. *Surf. Coat. Technol.* 203 (10–11), 1429–1437. doi:10.1016/j.surfcoat.2008.11.017

Cinca, N., and Guilemany, J. M. (2012). Thermal spraying of transition metal aluminides: An overview. *Intermetallics* 24, 60–72. doi:10.1016/j.intermet.2012.01.020

Ciulli, E. (2019). Tribology and industry: From the origins to 4.0. *Front. Mech. Eng.* 5, 1–12. doi:10.3389/fmech.2019.00055

Darmawan, A. S., Purboputro, P. I., Sugito, B., Febriantoko, B. W., Yulianto, A., Suprapto, S., et al. (2022). Increasing hardness and corrosion resistance of commercially pure titanium by using plasma nitrocarburizing process. *Acta Metall. Slovaca* 28 (1), 14–18. doi:10.36547/ams.28.1.1266

Djanarthany, S., Viala, J., and Bouix, J. (2001). An overview of monolithic titanium aluminides based on Ti3Al and TiAl. *Mat. Chem. Phys.* 72, 301–319. doi:10.1016/s0254-0584(01)00328-5

Gao, J. Y., Wang, L. J., and Jiang, W. (2013). Mechanism of Self-Propagating High-Temperature Synthesis of MoSi₂ . *Mat. Sci. Forum* 745–746, 587–593. doi:10.4028/www.scientific.net/msf.745-746.587

Gao, H., He, Y., Zou, J., Xu, N., and Liu, C. T. (2013). Pore structure control for porous FeAl intermetallics. *Intermetallics* 32, 423–428. doi:10.1016/j.intermet.2012.08.030

Gupta, S. P. (2002). Intermetallic compounds in diffusion couples of Ti with an Al–Si eutectic alloy. *Mat. Charact.* 49 (4), 321–330. doi:10.1016/s1044-5803(02)00342-x

Hai-xin, L. I., Peng, H. E., Tie-song, L. I. N., Feng, P. A. N., Ji-cai, F., and Yu-dong, H. (2012). Microstructure and shear strength of reactive brazing joints of TiAl/Ni-based alloy. *Trans. Nonferrous Metals Soc. China* 22, 324–329. doi:10.1016/s1003-6326(11)61178-3

Kobashi, M., Inoguchi, N., and Kanetake, N. (2010). Effect of elemental powder blending ratio on combustion foaming behavior of porous Al–Ti intermetallics and Al3Ti/Al composites. *Intermetallics* 18 (5), 1039–1045. doi:10.1016/j.intermet.2010.01.034

Locci, a. M., Orrù, R., Cao, G., and Munir, Z. a. (2003). Field-activated pressure-assisted synthesis of NiTi. *Intermetallics* 11 (6), 555–571. doi:10.1016/s0966-9795(03)00043-8

Merzhanov, A. G. (1996). Combustion processes that synthesize materials. *J. Mat. Process. Technol.* 56. Elsevier, 222–243.

Mohd Yuhazri Yaakob, M. A. H., Saion, M. P., and Husin, M. A. (2020). Potency of natural and synthetic composites for ballistic resistance: A review. *ARSTech.* 1 (2), 43–55. doi:10.23917/arstech.v1i2.52

Moore, J. J., and Feng, H. J. (1995). Combustion synthesis of advanced materials: Part I. Reaction parameters. *Prog. Mat. Sci.* 39 (4–5), 243–273. doi:10.1016/0079-6425(94)00011-5

Morsi, K. (2001). Review: Reaction synthesis processing of Ni–Al intermetallic materials. *Mater. Sci. Eng. A* 299 (1–2), 1–15. doi:10.1016/s0921-5093(00)01407-6

Muhammad, I. H. S., and Haruna Shanono, I. (2021). Contact stress analysis of a spur gear using Lewis and Hertz theory. *ARSTech.* 2 (2), 41–46. doi:10.23917/arstech.v2i2.165

Orru, R., Cao, G., and Munir, Z. A. (1999). Mechanistic investigation of the field-activated combustion synthesis (FACS) of titanium aluminides. *Chem. Eng. Sci.* 54, 3349–3355. doi:10.1016/s0009-2509(98)00459-x

Riyadi, T. W. B., Sarjito, S., and Partono, P. (2016). The effect of compaction pressures on the microstructure and properties of NiAl/Ti formed by SHS process. *ARPN J. Eng. Appl. Sci.* 11 (10), 6615–6618.

Riyadi, T. W. B., Zhang, T., Marchant, D., and Zhu, X. (2014). Synthesis and fabrication of NiAl coatings with Ti underlayer using induction heating. *Surf. Coat. Technol.* 258, 154–159. doi:10.1016/j.surfcoat.2014.09.037

Riyadi, T. W. B., Zhang, T., and Sarjito, S. (2014). Microstructure and adhesion of NiAl/Al and NiAl/Ni coatings formed by SHS process. *Appl. Mech. Mat.* 660, 185–189. doi:10.4028/www.scientific.net/amm.660.185

Romanova, V., Dymnich, E., Balokhonov, R., and Zinovieva, O. (2020). Mechanical aspects of deformation-induced surface roughening in the presence of inclusions in a subsurface layer. Numerical modeling. *Front. Mech. Eng.* 6, 1–10. doi:10.3389/fmech.2020.00066

Salehi, M., Karimzadeh, F., and Tahvilian, A. (2001). Formation of Ti–Ni intermetallic coatings on carbon tool steel by a duplex process. *Surf. Coat. Technol.* 148, 55–60. doi:10.1016/s0257-8972(01)01330-5

Sauthoff, G. (2008). Basics of Thermodynamics and Phase Transitions in Complex Intermetallics, 1. London: World Sceintific.

Stolo, N. S., Liu, C. T., and Deevi, S. C. (2000). Emerging applications of intermetallics. *Intermetallics* 8, 1313–1320. doi:10.1016/s0966-9795(00)00077-7

Tay, B. Y., Goh, C., Gu, Y., Lim, C., Yong, M., Ho, M., et al. (2008). Porous NiTi fabricated by self-propagating high-temperature synthesis of elemental powders. *J. Mat. Process. Technol.* 202 (1–3), 359–364. doi:10.1016/j.jmatprotec.2007.09.037